LA-UR -91-905

LA-UR--91-905

DE91 009957

TITLE. GRUNEISEN-STRESS INDUCED ABLATION OF BIOLOGICAL TISSUE

AUTHOR(S). R. S. Dingus, X-1
R. J. Scammon, WX-11

SUBMITTED TO International Society for Optical Engineering (SPIE)
OE/LASE '91 Biomedical Optics '91 Symposium
Laser-Tissue Interaction II Conference
Los Angeles, CA
January 20-25, 1991

DISCLAIMER

Los Alamos National Laboratory
Los Alamos, New Mexico 87545

Grüneisen-stress induced ablation of biological tissue

R. S. Dingus and R. J. Scammon
Los Alamos National Laboratory, Los Alamos, NM 87545

ABSTRACT

The objective of biomedical applications of lasers is frequently to remove tissue in a controlled manner. However, for ablation induced by thermal- or photo-decomposition, damage to surrounding tissue may be excessive in some instances. Tissue can also be ablated by a hydrodynamic process referred to as front surface spallation, in which a thin layer next to a free surface is heated to levels, below vaporization but, so rapidly that it cannot undergo thermal expansion during laser heating. This generates a stress pulse, which propagates away from the heated region, with an initial amplitude that can be calculated using the Grüneisen coefficient. As the pulse reflects from the free surface, a tensile tail can develop of sufficient amplitude, exceeding the material strength, that a layer will be spalled off, taking much of the laser-deposited energy with it. Because tissue is generally a low strength material, this process has the potential of producing controlled ablation with reduced damage to the remaining tissue. However, to achieve these conditions, the laser pulse length, absorption depth and fluence must be properly tailored. This paper presents hydrodynamic calculations and analytical modeling relating to both stress- and thermal-induced ablation as a function of laser and tissue properties to illustrate the potential benefits of stress induced ablation. Also, guidance is given for tailoring the exposure parameters to enhance front surface spallation.

1. INTRODUCTION

A mechanism for ablation of tissue is discussed that involves front surface spallation induced by Grüneisen-stress associated with short-pulse laser heating. For the sake of discussion, laser induced front surface spallation is referred to as photospall ablation. The photospall ablation process is described in graphical terms and is compared with other ablation processes. Equations are presented for predicting the effect and the region of parameter space for which it should occur along with specific predictions. Potential advantages of photospall are enumerated along with possible complications and limitations.

The term photoablation is used to refer to the surgical removal of tissue by lasers by any physical means. In order to put photospall in perspective, it is helpful to briefly discuss other photoablation processes; namely, photothermal and photochemical decomposition.

Photothermal decomposition refers to ablation by vaporization resulting from heating the tissue to high temperatures. At moderate laser intensities, where the front surface is cooled by vaporization, inner material can be superheated, leading to explosive vaporization at some depth, which also ejects non-vaporized outer material. Vaporization requires the large investment by laser deposition of the latent heat of vaporization, which leads to relatively high fluences. Also, it leaves a large residual heat in the tissue because the surface is left at the boiling temperature. At high intensities, a stress pulse of significant amplitude will be driven into the material by the rapid vapor departure. At even higher intensities, the vapor will be further heated by the laser to cause ionization. The ionized region will generally become highly absorptive because of the large inverse bremsstrahlung cross section producing a high temperature plasma with strong thermal radiation from this region. There are many potential damage mechanisms to surrounding tissue at these high intensities.

Photochemical decomposition is caused by absorption of photons by molecules resulting in the breakage of chemical bonds. Short wavelength lasers are required and precise, uniform ablation surfaces have been observed. Similarly, as for thermal decomposition, this process requires relatively high fluences because of the required investment of the heat of chemical formation, which is of similar magnitude to the latent heat of vaporization; although subsequent chain reactions can occur that result in a large quantum yield (number of molecules fragmented per incident photon). Large fluence at low flux (intensity) would not necessarily be a problem; unfortunately, much of the potential advantage of photochemical decomposition seems to be compromised by the fact that experience indicates that relatively high intensities are required for practical applications, reportedly because of competition with non decomposition relaxation processes. At the high intensities presently in vogue[1] to invoke photochemical ablation, photothermal decomposition also comes into action along with the associated damage mechanisms to surrounding tissue discussed above. It appears that, for the advantages of the photochemical decomposition process to be fully realized, techniques for its application at low intensity must be found.

Front surface spallation (or photospall) is another potential mechanism by which to achieve photoablation. With this process, layers of tissue are ejected without vaporization, and therefore (for a given laser absorption depth) at lower fluences

than for photo-thermal or -chemical ablation. The residual tissue temperature is low with this process so that it should provide reduced damage to surrounding tissue. Optimally, the laser pulse length needs to be less than or about equal to the time for an acoustic signal to traverse one laser absorption depth.

2. PHOTOSPALL PROCESS

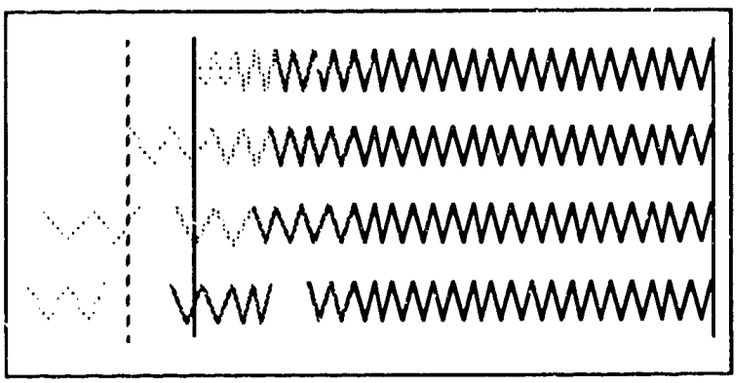

Figure 1. Illustration of front surface spallation process.

Figure 1 illustrates the basic process relating to front surface spallation. Imagine that the tissue of interest is a spring with a certain compressibility; fig. 1 shows four configurations of this spring. Suppose that the front surface of the tissue (spring) is heated to some depth during a short time as illustrated by the hatched portion of the spring at the top in the figure. If the material had been heated slowly, thermal expansion would have caused it to expand to the vertical dotted line to the left in Fig. 1, as shown in the next spring down. However, because it was heated so rapidly, it acquires a significant velocity during the expansion, which must be followed by deceleration to bring it back to rest. If the tissue has insufficient strength, the force associated with the deceleration will cause a fracture and a layer will keep going as shown by the next case. This fracture is referred to as spallation, or spall for short. Depending on the circumstances, the velocity of the residual tissue can cause one or more additional layers to spall as shown for the bottom spring.

Front surface spallation for tissue can also be described in more quantitative, but equivalent terms. Heating a (front surface) layer of tissue before it can thermally expand causes a (positive) compressive stress pulse in that region whose amplitude can be calculated using the Grüneisen coefficient. This stress pulse will cause dynamic expansion, both toward the front surface and in the opposite direction. The stress pulse will be reflected at the front surface by the shock impedance mismatch producing a reflected (negative) tensile pulse, if the impedance of the material in front is less than that of the tissue. To have spall, it is generally necessary that the material in front of the tissue be a gas or vacuum and not a liquid or solid; otherwise, the shock impedance of the material in front will prevent a tensile wave of sufficient amplitude from developing. This would seem to imply that photospall could not be used for laser angioplasty because of the blood or saline solution in contact with the plaque to be removed; however, this shock impedance problem might be eliminated by preceding the photospall laser pulse with a laser prepulse that would be absorbed in the liquid in front of the plaque to create a (low shock impedance) transient vapor bubble (Steve Jacques has demonstrated that such a vapor bubble can be created using a Ho:YAG laser pulse transmitted through an optical fiber into water[2]). The tensile pulse trails the compressive pulse into the tissue, thus causing the characteristic bipolar stress pulse seen in stress measurements at low fluences [1]. If at some depth, the tensile stress exceeds the tensile spall strength of the tissue, then the tissue will spall at that depth, creating a new boundary surface at which the stress becomes zero. The rest of the compressive pulse that is propagating toward the front surface will then be reflected from this new boundary. If the reflected tensile stress builds up to the spall stress again, then spall will occur again. Eventually, the criterion will no longer be met for another spall layer to develop and a residual tensile tail will be left in the tissue with an amplitude that is less than the spall strength of the tissue.

2. PHOTOSPALL RELATIONS

To understand the basic relations governing the photospall process, a purely thermoelastic response of the tissue is assumed along with an exponential laser deposition profile. For the large absorption coefficient, μ, and small depth, x, of interest in the tissue, it should be a reasonable approximation to neglect scattering of the laser beam and to assume thermoelastic response. For the sake of discussion, except when specifically noted otherwise, it is assumed that the deposited laser energy is instantly converted into heat; there have been speculations that this may not always be a good assumption[1]. The time scale is assumed to be short enough that thermal conduction can be ignored, however, it is assumed that the heat is distributed locally uniformly where it is deposited (which may or may not be a good assumption for

heterogeneous tissue with laser absorption in one constituent). The laser beam is assumed to expose a large diameter of tissue compared to the absorption depth; even with this assumption, there is likely an important issue with regard to tearing around the periphery of the spall layer, which is discussed in Section 5.

For an incident fluence F_0 into the tissue (after correction for reflection at the tissue surface), the fluence, F, at a depth x in the tissue is given by

$$F = F_0 \exp(-\mu x) \quad . \tag{1}$$

The energy density (energy per unit mass), E, deposited by the laser in the tissue at depth x is

$$E = -(1/\rho)\, dF/dx = (\mu/\rho)\, F_0 \exp(-\mu x) \quad . \tag{2}$$

A rectangular step function laser temporal profile is assumed with a pulselength, t_L, because it is most illustrative. Only the pulselength is fundamentally important to the process; for temporal profiles involving a more complex pulse shape such as a finite rise time and decay time, the analysis is still generally applicable with minor modification.

The material properties important to the photospall process are: the absorption coefficient, μ; the sound speed, c; the Grüneisen coefficient, Γ; and the spall strength, σ_s. It is convenient to define a characteristic time , t_0, where

$$t_0 = 1 / \mu c \quad , \tag{3}$$

which is the time for an acoustic signal to propagate a distance of one laser absorption depth ($1/\mu$). Also, let τ_L be the ratio of the laser pulselength to this characteristic time, so

$$\tau_L = t_L / t_0 = \mu c\, t_L \quad . \tag{4}$$

It is instructive to discuss how the stress waveform develops in the tissue. For simplicity, the sound speed is assumed to be constant (actually at higher compressive stress, the speed is generally slightly higher, but this change is probably negligible for the low stresses and short distances of interest in the present discussion). If the laser energy was deposited instantaneously in the tissue, the stress, σ, in the tissue just after deposition would be compressive with an amplitude at a distance x into the tissue of

$$\sigma = \Gamma \mu F_0 \exp(-\mu x) \quad . \tag{5}$$

Actually, because the front surface is a free surface (it is assumed that air, which has a shock impedance of essentially zero, is outside the front surface), the stress must be zero for all time at x = 0; this boundary condition is insured by the ensuing reflection at this surface. The stress pulse immediately begins to propagate both toward the surface and away from the surface with a velocity c. This bifurcation in direction, leads to a factor of two reduction in amplitude. For illustrative purposes, one can think of the stress given in Eq. 5 as consisting of two pulses, each with half the amplitude of Eq. 5; one moving inward, the other outward. At any given time, the stress is the superposition of these two pulses. The inward moving pulse simply translates with velocity c. Each element of the outward moving pulse reverses sign and direction as it reflects from the front surface. This results in a bipolar stress pulse, which, at any given time t, makes an abrupt transition at the location ct in the tissue from the largest tensile value to the largest compressive value. For times of the order of or less than the characteristic time, t_0, the peak tensile stress is building asymptotically from zero to its maximum negative value of $\Gamma\mu F_0/2$, while the peak compressive stress is decreasing asymptotically from $+\Gamma\mu F_0$ to $+\Gamma\mu F_0/2$. During times for which $t >> t_0$, the stress amplitude decreases from the peak stress value, σ_p, to zero exponentially as $\exp(-\mu|x'|)$ in both directions, where $|x'|$ is the distance from the location ct. Because of the assumed linear elastic behavior, similar statements could be made regarding the stress as a function of time at given positions in the tissue. It is interesting to note that nowhere in this paper are the processes under discussion dependent on a shock front[3] developing in the tissue.

If the laser has a finite pulselength, t_L, then stress propagation occurs during the pulse causing a number of differences from instantaneous energy deposition. For a rectangular step function laser temporal profile (as is being assumed), the tensile stress does not begin to develop until the laser pulse ends. During times for which $t >> t_0$, and $t >> t_L$, the tensile

and compressive stress peaks become separated by a distance ct_L and the peak stress value, σ_p, is reduced by a factor A, which accounts for the stress relief that occurs during the laser pulse, where

$$A = (1 - \exp(-\tau_L)) / \tau_L \quad . \tag{6}$$

This attenuation factor approaches 1 as τ_L goes to zero and approaches $1 / \tau_L$ for large values of τ_L. The factor A is plotted versus τ_L in Fig. 2. As illustrated in Fig. 2, the peak stress is reduced substantially when τ_L is greater than one.

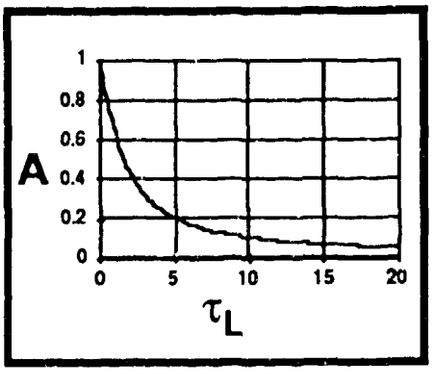

Figure 2. Stress attenuation versus ratio of laser pulselength to characteristic time.

Thus, the peak tensile stress , σ_p, developed in the tissue occurs (assuming no spall) at times late compared to the laser pulse duration, t_L, and late compared to the characteristic time, t_0, and has an amplitude of

$$\sigma_p = (A/2)\, \Gamma\, \mu\, F_0 \quad \text{for } t >> t_L \text{ and } t >> t_0 \quad . \tag{7}$$

It is interesting to note that, when $\tau_L >> 1$, then σ_p is inversely proportional to t_L and independent of μ; that is,

$$\sigma_p = (1/2)\, \Gamma F_0 / (ct_L) \quad \text{for } t >> t_L \ , \ t >> t_0 \text{ and } \ \tau_L >> 1 \quad . \tag{8}$$

To better understand the origin of the stress, it is helpful to examine the terms in Eq. 7. The Grüneisen coefficient can be written as

$$\Gamma = \beta / (\rho\, C_v\, \kappa_T) \tag{9}$$

where β is the thermal expansion coefficient, ρ is the density, C_v is the specific heat at constant volume and κ_T is the isothermal compressibility of the tissue. Putting this expression into Eq. 7 gives

$$\sigma_p = (A/2)\, (1/\kappa_T)\, \beta\, (\mu/\rho)\, F_0 / C_v \quad . \tag{10}$$

The product $(\mu/\rho)F_0$ gives the peak laser dose in energy per unit mass, which occurs at the front surface of the tissue; dividing this by C_v gives the temperature rise; multiplying this by β gives the thermal expansion; multiplying this by $1/\kappa_T$ gives the stress caused by this thermal expansion; multiplying this by 1/2 accounts for the stress propagating both inward and outward as discussed above; and multiplying this by A corrects for stress propagation during the laser pulse.

Equation 7 assumes a Mie Grüneisen equation of state, which is applicable for the solid and liquid phases. At high fluences where vaporization occurs, as the vapor expands, the equation of state more nearly approximates that of an ideal gas. At such high fluences, Eq. 7 is no longer valid because the phase change to a gas causes a much different material expansion process. The pressure applied to the solid/liquid surface by the expanding gas tends to suppress the tensile stress pulse discussed above. The criterion for vaporization is that the front surface dose (given by $(\mu/\rho)F_0$) exceeds incipient vaporization enthalpy, ΔH_v, i.e., the enthalpy required to raise the tissue temperature from its ambient value to the

vaporization temperature. Thus, Eq. 7 begins to become invalid when the fluence is above the value limited by

$$(\mu/\rho)F_0 < \Delta H_i \quad . \tag{11}$$

To convert the tissue completely to a vapor requires an additional enthalpy, ΔH_v, which is the latent heat of vaporization, in addition to ΔH_i; so the complete vaporization enthalpy, ΔH_c, is

$$\Delta H_c = \Delta H_i + \Delta H_v \quad . \tag{12}$$

The quantity ΔH_v is generally large compared to ΔH_i. Only a fraction of the material with a dose between ΔH_i and ΔH_c will be vaporized; however, even though not vaporized, material with a dose in this range can be driven off by the fraction that is vaporized; whether this non-vaporized material is actually driven off depends on the dynamics.

In reality it takes a finite time for materials to fracture when subjected to a tensile stress and fracture models have been developed to account for this complication[4], which may or may not be consequential for photospall of tissue. Neglecting this complication for now, if the spall strength of the tissue is less than the peak tensile stress, then the tissue will spall at the location and time in the tissue where and when the peak stress reaches the spall strength. Thus, spall occurs if

$$\sigma_p > \sigma_s \quad . \tag{13}$$

After the spallation occurs, depending on the circumstances, the tensile stress may build again to the spall strength amplitude, spalling off another layer. The total number of spall layers is approximately one to two times the ratio σ_p / σ_s and the total spall depth is approximately one to a few times the laser absorption depth ($1/\mu$). These relations for the number of spall layers and the spall depth are not exact principally because part of the tensile stress pulse generally will have propagated beyond the spall location by the time of each spall and because of the discrete nature of the spallation process in association with an exponentially increasing stress with distance into the tissue.

3. ANALYTIC STRESSWAVE CALCULATIONS

Figures 3 and 4 present the results of calculations of the purely thermoelastic response of tissue, assuming that the spall strength is large enough that spall does not occur, based upon equations given in the Appendix derived from a paper by Bushnell[5] for a rectangular step function laser temporal profile. In Fig. 3, the material properties used are those estimated for tissue exposed to a typical ArF laser pulse as has been used for corneal ablation. Figure 4 is for the same conditions except that the laser pulselength is 1 ns instead of 16 ns.

In the top part of Figs. 3 and 4, the stress in the tissue is plotted as a function of time at different positions in the tissue. The bottom part of Figs. 3 and 4 gives the stress as a function of position in the tissue at different times. In these figures, it may be noted that the separation between the positive and negative peaks is equal to the pulse length, that no negative stress develops during the laser pulse and that the peak stress amplitude is much larger for the 1 ns pulse than for the 16 ns pulse as indicated by Eq. 7.

4. HYDRODYNAMIC CODE CALCULATIONS

Figures 5 and 6 present the results of hydrodynamic calculations, using the Chart D code[6] with the laser and material properties shown in those figures, to illustrate how the stress behavior changes when front surface spall occurs. The equation of state used was approximately that for aluminum, but it was artificially changed for illustrative purposes. In Fig. 5, a large spall strength was used so that spall would not occur; the stress is plotted in dynes/cm^2 (10^6 dynes/cm^2 = 1 bar) as a function of position in the material at times of 1.59 ns, 1.90 ns, 10 ns and 20 ns. In these plots the front surface was at x = 0.2 cm and x decreases as the distance into the material increases. In Fig. 6, where a spall strength of 3 kbar was used, the stress is plotted at essentially these same times plus at two additional times. The dashed vertical lines in Fig. 6 indicate the location at which spall planes develop. Spall first occurs at a time of 1.54 ns when the tensile stress reaches 3 kbar. The plot at 1.90 ns shows that the tensile stress has again built up to nearly 3 kbar. The plot at 1.92 ns shows that a second spall plane has developed. At 10 ns, six spall planes have developed and another is about to occur. At 10.9 ns, the seventh and last spall plane has occurred. After spall, the residual stress pulse in each spall layer reflects repeatedly within that layer. The momentum of each spall layer is about the same, but the thickness increases exponentially with successive layers so that the velocity decreases exponentially with successive layers. This signature might be something to look for experimentally. The position, x, in Figs. 5 & 6 is a Lagrangian coordinate (which is fixed to the mass elements rather than representing location in space) so that the gaps between spall layers do not appear in the plots.

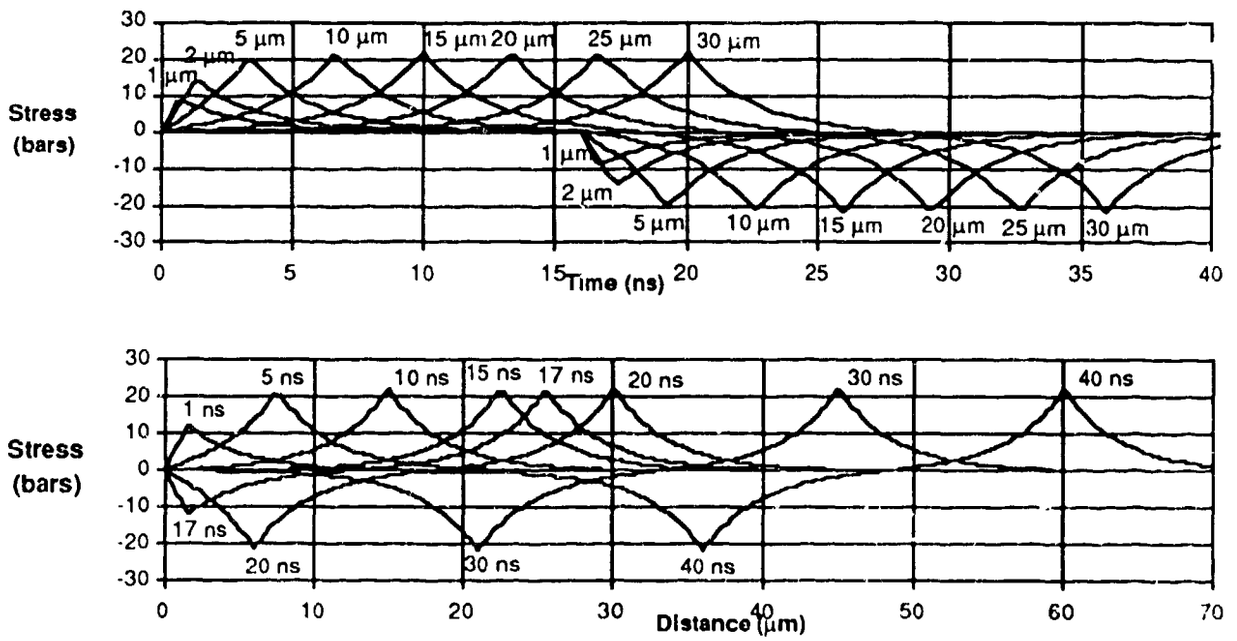

Figure 3. Thern oelastic stresswave development for long laser pulselength compared to characteristic time. Parameters used were: $\mu = 2700\ cm^{-1}$, c = 1.5 μm/ns, Γ = 0.15, $F_0 = 0.07\ J/cm^2$, t_L = 16 ns. Resultant values are: $\tau_L = 6.5$, $\sigma_p = 22$ bar and front surface temperature rise is 45 °C.

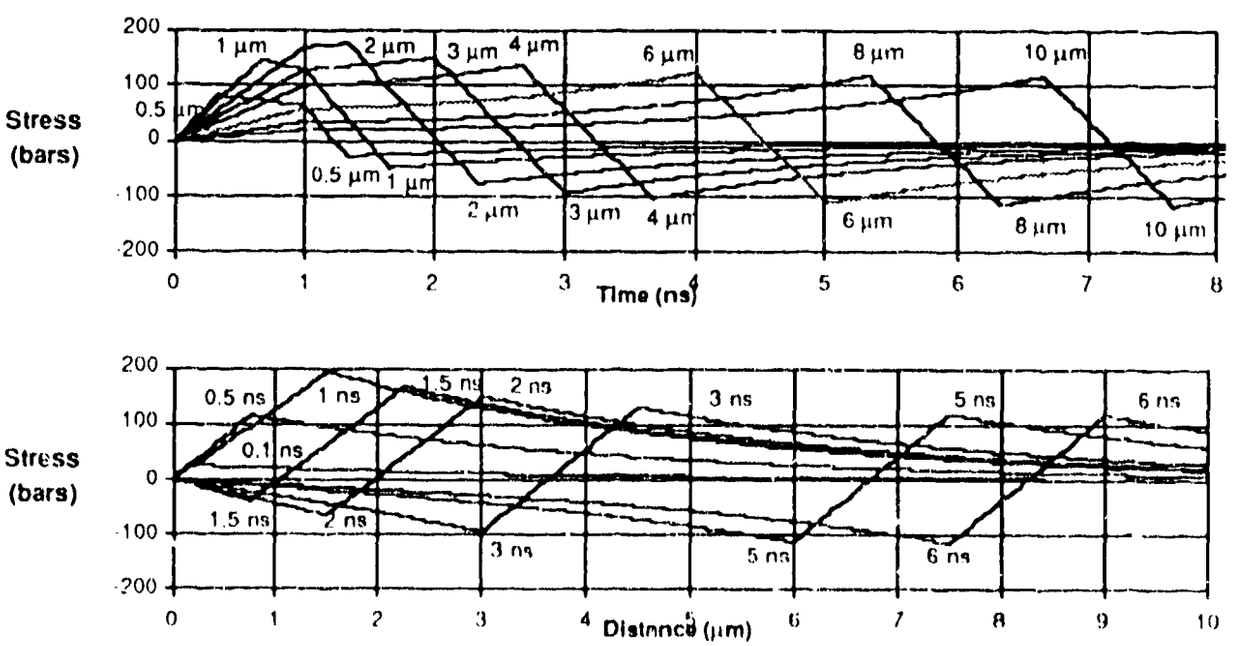

Figure 4. Thermoelastic stresswave development for short laser pulselength compared to characteristic time. Parameters used were: $\mu = 2700\ cm^{-1}$, c = 1.5 μm/ns, Γ = 0.15, $F_0 = 0.07\ J/cm^2$, t_L = 1 ns. Resultant values are: $\tau_L = 0.41$, $\sigma_p = 117$ bar and front surface temperature rise is 45 °C.

APPROXIMATE ALUMINUM EOS
artificial parameters
for illustrative purpcses

μ = 300 cm^{-1} Γ = 2.5 t_L = 0.65ns
c = 5.17 μm/ns F_0 = 3.6 J/cm^2 τ_L = 0.1 Spall Strength = ∞

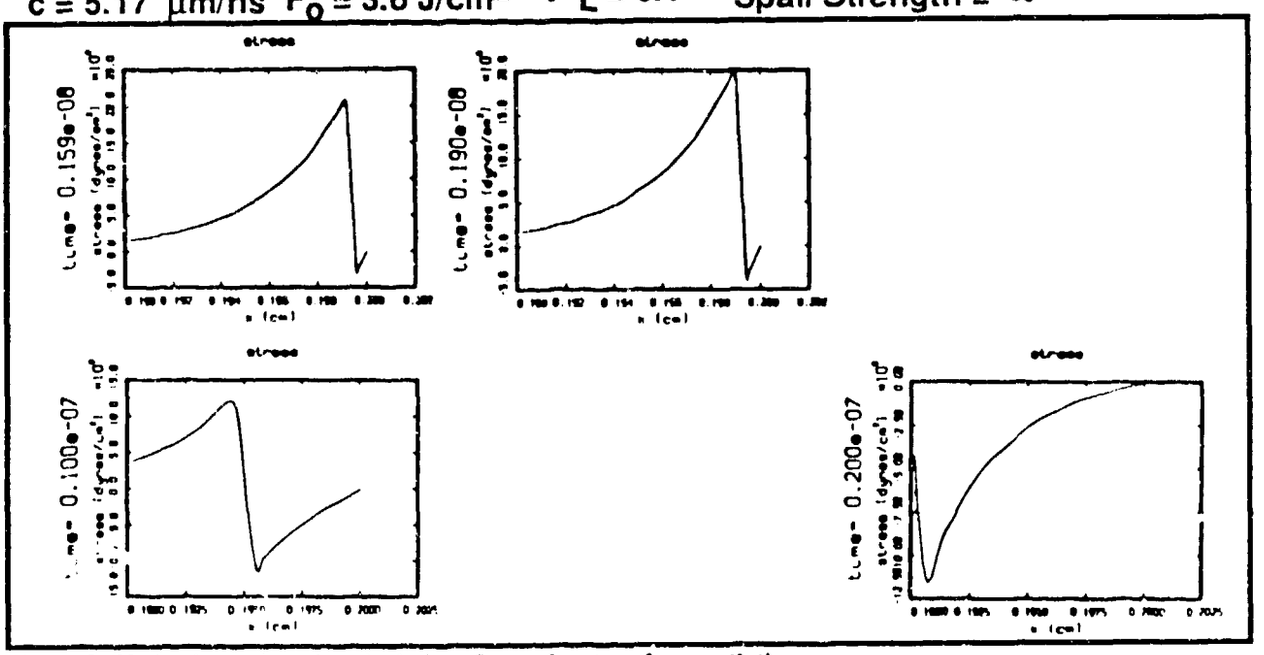

Figure 5. Hydrodynamic code calculations for no front surface spallation.

APPROXIMATE ALUMINUM EOS
artificial parameters
for illustrative purposes

μ = 300 cm^{-1} Γ = 2.5 t_L = 0.65ns
c = 5.17 μm/ns F_0 = 3.6 J/cm^2 τ_L = 0.1 Spall Strength = 3 kbar

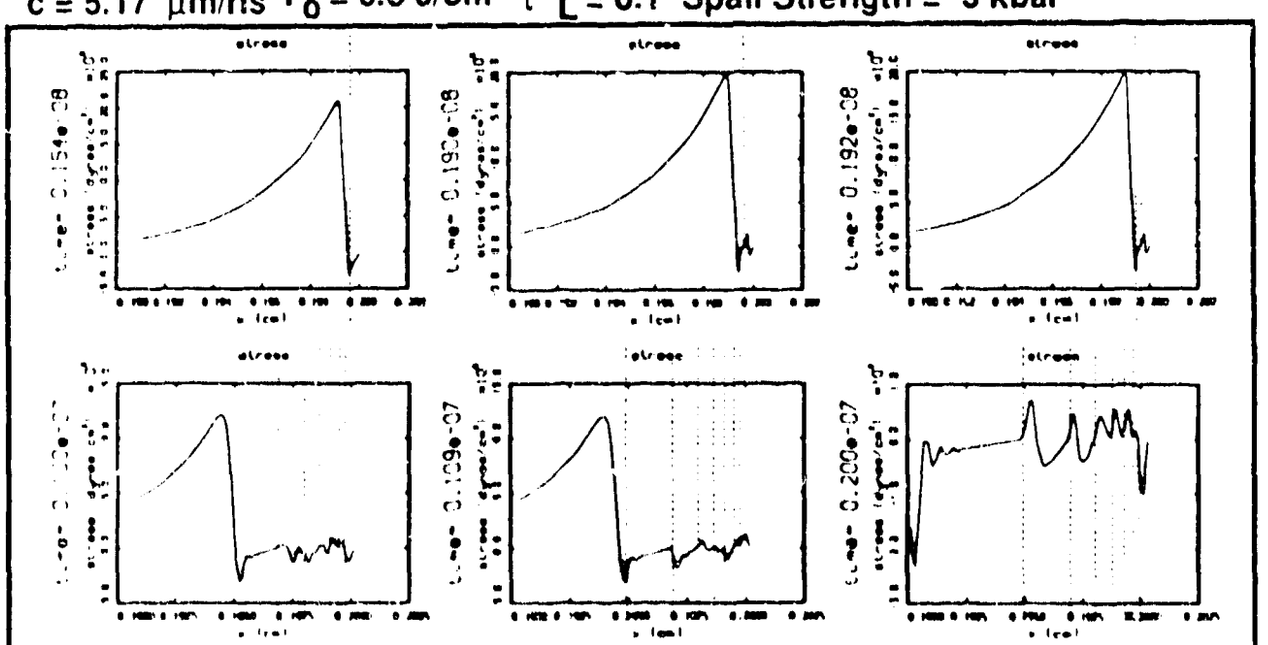

Figure 6. Hydrodynamic code calculations for with front surface spallation.

5. ESTIMATED PROPERTIES AND ANALYSES

Whether photospall can be invoked for medical applications will depend largely on tissue and laser properties. A cursory examination of the approximate properties will now be done in order to estimate the threshold for photospall as well as the threshold for vaporization, which is to be avoided as indicated earlier. The values presented here are intended for estimating whether the process will occur in a practical sense. Because a large fraction of tissue is water, guesses of tissue properties will sometimes be based on estimates for water.

The incipient vaporization enthalpy for water is in the vicinity of 400 J/g (depending on the ambient temperature) and the complete vaporization enthalpy is about 2700 J/g. As indicated by the discussion above and Eq. 11, the objective is to achieve photospall with irradiations for which the front surface dose is considerably less than this value of 400 J/g, in order to minimize thermal, as well as stress, damage to surrounding tissue.

The speed of sound in water is about 1.5 μm/ns and should be well known for tissue because of ultrasound work. The Grüneisen coefficient for water is about 0.3; soft tissue might have a similar value. However, it should be noted that the effective Grüneisen coefficient is reduced substantially by even a slight degree of porosity; it would seem important to keep the tissue saturated with water during photospall operations to avoid porosity. Determination of the Grüneisen coefficient can be made by measuring the density, specific heat, thermal expansion coefficient and compressibility and calculating the coefficient from Eq. 9. A more accurate determination of Γ can probably be achieved from stress measurements for dynamic experiments such as laser exposure and comparison of results with Eq. 7. The Grüneisen coefficient is not strictly a constant (causing Eq. 7 to be only an approximate relation); so that experimental determinations of the parameter should be designed to measure its variation over the range of interest. Neglecting reflection of the incident fluence at the tissue surface (which may introduce some error), comparison of calculations using Eq. 7 with stress amplitude measurements by Dyer[1] for cornea irradiated with a KrF laser (with a pulselength that was apparently about 10 to 20 ns) indicate a value for the Grüneisen coefficient of about 0.15 for fluences below the ablation threshold, which was observed to be at 0.15 J/cm^2.

Depending on the laser wavelength, the laser absorption coefficient, μ, of the tissue can vary from small values up to about 12,000 cm^{-1}. To promote photospall, the pulselength, t_{L_s} needs to be sufficiently short; specifically, the product $\mu c t_{L_s}$ needs to be less than or about one in order to keep the quantity A near one. There seem to be advantages to selecting a large absorption coefficient (and thus a short pulselength) for photospall such as minimizing the fluence per pulse and minimizing the impulse (momentum) per pulse. Also, for short pulselength, the residual compressive stress pulse will rapidly attenuate due to dispersion as it propagates through the tissue, which should reduce stress damage to the remaining tissue. However, there might be circumstances where lower absorption coefficients and longer laser pulselengths would be preferred. For example, at high flux and/or high repetition rate, laser pulse blockage by tissue fragments from previous pulses or aerosol breakdown might occur; this might impose limitations on the flux or repetition rate or dictate special gas handling procedures over the tissue in the exposure region.

The spall strength is probably the parameter with the largest uncertainty and could be the determining factor as to whether photospall can be utilized in medical applications. The spall strength for water, resulting from surface tension and viscosity, is reported[7] to be about 2 to 20 bar, with expected dependence on strain rate. In general, the spall strength of a material is strain rate and temperature dependent; this potential complication, which may or may not have practical consequences for medical applications, should be taken into consideration when interpreting experimental data. The spall strength of water would seem to set a lower limit for the spall strength of tissue. Perhaps for soft tissue the bonds between cells or fibers is not large so that it is conceivable that in certain regions and in certain directions, the spall strength of tissue is not much larger than that of water. Also, it seems plausible that photodecomposition might reduce the spall strength so that a combination of photospall and photodecomposition might be effective; in other words, it might be effective to use short wavelength lasers for photospall.

In the KrF laser irradiations of cornea by Dyer[1] discussed above, the absorption coefficient is reported to be 330 cm^{-1} with the ablation threshold at 0.15 J/cm^2 where the stress amplitude is 22 bar. Putting this absorption coefficient and fluence into Eq. 2 gives a front surface energy density at the ablation threshold of only 50 J/g, which corresponds to a temperature rise of about 12 °C, well below the threshold for photothermal ablation. It appears likely that photospall is the mechanism for photoablation in these experiments and that, based upon this data, the spall strength of the cornea is about 20 bar. It has been reported[1, 8] that ablation with 248 nm radiation produced incisions with ragged edges and more severe damage in adjacent stroma than with 193 nm; this would seem to be (at least partially) a natural consequence of the large absorption depth for KrF compared to ArF. For very thin spall layers, perhaps each one would break away cleanly around the periphery. However, with a large absorption depth in soft tissue, a spall layer with a thickness of a few tens of microns

would be expected, which might be so thick that it would not break free cleanly around the periphery. With multiple pulses in rapid succession, perhaps the first laser pulse would produce a spall plane and the next pulse would produce mid-plane spall in the previously spalled layer (because of stresswave reflection at the spall plane), etc. until the layer was finally eroded away; this would surely be an undesirable approach, likely leaving a jagged edge and possibly spall planes at greater depth. Further experiments and analysis should be able to establish whether this speculative explanation is correct; for example, it might be useful to look for a spall plane after a single laser irradiation pulse.

Stress amplitudes have been measured by Dyer[1] for cornea exposed to 16 ns ArF pulses. Based upon the ArF low intensity absorption coefficient of 2.7×10^3 cm^{-1}, the characteristic time, t_o, is about 2.5 ns. Because of the long ArF pulselength relative to the characteristic time, the peak stress can be calculated from Eq. 8, instead of Eq. 7. The measured stress has about the same value as the peak stress calculated using a Grüneisen coefficient of 0.3 with Eq. 8 for fluences above about 0.2 J/cm^2 (although this is in the vaporization regime where Eqs. 7 and 8 began to become questionable as discussed above). At lower fluences, the measured value falls off rapidly, with there being no measurable stress below 0.05 J/cm^2. Above 0.05 J/cm^2, the stress pulse is unipolar (compressive) and ablation starts at this fluence. Eq. 2 gives a front surface dose at this fluence (neglecting reflection at the tissue surface) of about 130 J/g (corresponding to a 30 °C temperature rise, assuming rapid conversion to heat), which is well below the vaporization threshold. Based upon an assumed enthalpy of 400 J/g, incipient vaporization would be about 0.13 J/cm^2; above this fluence photothermal decomposition would play a major roll in the photoablation process. At fluences above 0.07 J/cm^2, the measured peak stress is above 20 bar, where (based upon the KrF data discussed above) photospall would be expected. Perhaps photochemical decomposition is playing a roll to weaken the tissue to reduce the spall strength to lower than 20 bar and cause ablation to begin at the reported 0.05 J/cm^2 value.

The curious behavior for ArF is the nonlinear decrease of the stress to zero between 0.2 and 0.05 J/cm^2. There has been speculation[1], that this might be caused by the photochemical absorption of the laser photons leading to long lived (compared to the laser pulselength) excited states, thus delaying the conversion of deposited energy to heat, which would inhibit photospall in the same manner as a long pulselength laser does. This could be accounted for by putting this excited-state lifetime into Eq. 8, instead of the pulselength, t_L; however, to match the data, this lifetime would have to decrease from a large to a small value as the fluence increases from 0.05 to 0.2 J/cm^2, which would imply that the threshold for some mechanism for deexcitation is being reached in this fluence range. Knowing how this nonlinear behavior depends on laser flux and material temperature would also be valuable. It is also plausible that a small degree of porosity could cause a small effective Grüneisen coefficient until enough thermal expansion has occurred to fill the pores; however, this seems to be discountable because the measurements for exposures of cornea to KrF lasers did not show this nonlinear stress behavior at low fluences. Further experiments, and supporting analyses, such as time resolved stress, temperature and fluorescence measurements as a function of laser pulse length and fluence should provide a definitive resolution of this issue. The issue seems important to resolve because it affects all mechanisms for ablation as well as secondary damage to surrounding tissue.

Although it appears that photospall occurs for KrF irradiation of cornea, the large absorption depth seems to be a disadvantage. The absorption depth is much smaller for ArF. If the ArF pulselength could be reduced from the present value of about 16 ns to about 1 ns, then, at least above 0.05 J/cm2, photospall could be enhanced as an ablation mechanism for this wavelength laser. By selecting a laser with a short pulselength and with a wavelength where the absorption coefficient but where the generation of heat is not delayed by the decay times of states excited by photochemical absorption, then ablation might be accomplished with photospall at lower fluences and lower temperatures than presently needed with ArF lasers. For example, corneal ablation might be achieved by photospall with a pulselength of about a nanosecond at a wavelength near 3 μm where the absorption coefficient of water is large; by tailoring the wavelength and pulselength in relation to the water absorption peak near 3μm, perhaps the optimum ablation conditions could be found.

In further considerations of photospall for medical applications, it would seem appropriate to first perform experiments with judicious diagnostics under conditions dictated by equations in Section 2, using estimated or best available material properties to confirm the validity of the photospall relations. Initial experiments might best utilize simple materials such as water or polymers to demonstrate the physical principals. Diagnostics might include: pressure, impulse, ablation depth and high speed photographic measurements. If these results show prospect, it might then be appropriate to continue these same type of experiments on biological tissue with careful, systematic variation of appropriate parameters in order to deduce the tissue properties needed in the equations. Having verified the physical relationships and obtained necessary material properties, calculations could then be performed to provide accurate guidance of laser parameters to be used in clinical applications.

6. SUMMARY

In summary, to take advantage of the potential benefits of the photospall process, the pulselength needs to be about equal to or shorter than the time for an acoustic signal to traverse one laser absorption depth. The applicability of photospall to medical practice basically depends on whether the ratio of the Grüneisen coefficient to the spall strength is sufficiently large; there may also be an issue with how the spall layer breaks away around the periphery of the exposed area of tissue. It appears that this ratio likely is large enough so that, for short pulse lengths, spallation would occur at fluences well below thermal vaporization, in which case photospall should be an effective mechanism for photoablation of tissue for medical applications and thermal damage of the remaining tissue should be reduced with this process. For example, if $\Gamma \geq 0.15$ and $\sigma_s \leq 50$ bar, by using short pulselengths to invoke photospall, it should be possible to substantially reduce the residual temperature rise in the tissue compared to that associated with present corneal ablation techniques for which 10 to 20 ns pulselength ArF lasers at fluences above 100 mJ/cm^2 are needed. Also, by operating at just above the threshold for photospall, the compressive pulse imparted to the tissue can be limited to just above the absolute value of the tensile spall strength and this can be caused to attenuate rapidly as it propagates into the tissue by utilizing a short laser pulselength. This should further reduce the damage to the remaining tissue. Finally, when operating at a wavelength for which the absorption coefficient is about 10,000 cm-1 or larger, which occurs at about 3 μm for water, the laser pulse needs to be of sub-nanosecond duration. This might be an ideal application for a RF linac free electron laser, which could operate at this wavelength and has such a short pulse with a very high repetition rate.

7. APPENDIX--THERMOELASTIC STRESS FOR RECTANGULAR LASER PULSE

Let $\tau = \mu ct$, $\tau_L = \mu ct_L$, $\xi = \mu x$, and $A = (1 - \exp(-\tau_L)) / \tau_L$. Then, assuming that the laser flux is constant for a duration of t_L and with a total fluence of F_0, evaluating the integrals presented in the paper by Bushnell[5] gives:

$\sigma = (1/(2\tau_L))\, \Gamma\mu F_0\, [\exp-(\tau - \xi) - \exp-(\tau + \xi)]$ for $\tau \leq \tau_L$, $\xi \leq \tau$

$\sigma = (1/(2\tau_L))\, \Gamma\mu F_0\, [\exp-(\xi - \tau) - \exp-(\xi + \tau)]$ for $\tau \leq \tau_L$, $\xi \geq \tau$

$\sigma = -(A/2)\, \Gamma\mu F_0\, [\exp-(\tau - \xi - \tau_L) - \exp-(\tau + \xi - \tau_L)]$ for $\tau \geq \tau_L$, $\xi \leq \tau$, $\xi \leq \tau - \tau_L$

$\sigma = -(A/2)\, \Gamma\mu F_0\, [B\exp-(\tau - \xi - \tau_L) - \exp-(\tau + \xi - \tau_L)]$ for $\tau \geq \tau_L$, $\xi \leq \tau$, $\xi \geq \tau - \tau_L$

where $B = (\exp 2(\tau - \xi - \tau_L) - \exp(-\tau_L)) / (1 - \exp(-\tau_L))$

$\sigma = (A/2)\, \Gamma\mu F_0\, [\exp-(\xi - \tau) + \exp-(\xi + \tau - \tau_L)]$ for $\tau \geq \tau_L$, $\xi \geq \tau$

8. REFERENCES

1. P. E. Dyer and R. K. Al-Dhahir, *Transient photoacoustic studies of laser tissue ablation*, Proceedings of Laser-Tissue Interaction, SPIE Vol. 1202, 1990.

2. S. L. Jacques, private communication, 1991.

3. R. S. Dingus and B. P. Shafer, *Laser-induced shock wave effects in materials*, Proceedings of Laser-Tissue Interaction, SPIE Vol. 1202, 1990.

4. F. R. Tuler and B. M. Butcher, *A criterion for the time dependence of dynamic fracture*, J. of Fracture Mech. 4-4, 431-437, Dec, 1968.

5. J. C. Bushnell and D. J. McCloskey, *Thermoelastic stress production in solids*, J. Appl. Phys. 39, 5541-5546, 1968.

6. S. L. Thompson and H. S. Lauson, *Improvements in the CHART D Radiation Hydrodynamic Code II: A Revised Program*, SC-DR-710715, Sandia Laboratories, Albuquerque, NM, February 1972.

7. D. E. Grady, *The Spall Strength of Condensed Matter*, J. Mech. Phys. Solids 36:3, 353-384 (1988)

8. C. A. Puliafito, R. F. Steinert, T. F. Deutch, F. Hillenkamp, E. J. Dehm and C. M. Adler, *Excimer Laser Ablation of the Cornea and Lens*, Opthalmology, 92, 741-748, 1985.